Reactive Processing of LLDPEs in Corotating Intermeshing Twin-Screw Extruder. I. Effect of Peroxide Treatment on Polymer Molecular Structure

MARLY G. LACHTERMACHER* and ALFRED RUDIN†

Institute for Polymer Research, Department of Chemistry, University of Waterloo, Waterloo, Ontario, Canada N2L 3G1

SYNOPSIS

Commercial ethylene–octene linear low-density polyethylene (LLDPE) polymers were reactively extruded with low levels of 2,5-dimethyl-2,5 di(*t*-butylperoxy)hexane to modify their molecular structure and processing properties. Peroxide levels were kept low to avoid crosslinking. This article examines the effects of reactive extrusion in a corotating intermeshing extruder. Gel content analyses and examination of extruded thin tapes indicated that the products were gel-free, but line-broadening in high-resolution ^{13}C-NMR spectra suggested that some crosslinking did occur. Molecular weight distributions were broadened toward higher molecular weights, as expected. SEC estimates of long-chain branching in reacted polyethylenes were consistent with the results of ^{13}C-NMR analyses. Under our extrusion conditions, the products contained about one long branch per number-average molecule. This result and data on changes in carbon–carbon unsaturation indicate that the major chain extension mechanism is an end-linking reaction between terminal vinyls or allylic radicals formed at chain ends and secondary radicals. Both types are produced by hydrogen abstraction on the LLDPE. All long branches originated at tertiary branch points. Changes in thermal behavior, as measured by DSC analyses, paralleled those observed by temperature-rising elution fractionation (TREF). SEC molecular weight measurements and long-branch determinations by SEC and ^{13}C-NMR can be used to quantify the effects of peroxide treatment on the molecular structure of polyethylenes. DSC and TREF techniques, however, appear to be more sensitive than are SEC or NMR. Relatively minor variations in the degree of mixing and temperature control during reactive extrusion have noticeable effects on the molecular structures of the peroxide-treated LLDPEs. © 1995 John Wiley & Sons, Inc.

INTRODUCTION

In contrast to the low-density polyethylene (LDPE) processes, linear low-density polyethylene (LLDPE) is produced under moderate temperatures and pressures (60–200°C, 5–200 kg/cm^2) and has the advantage of lower capital and energy costs than does high-pressure, free-radical LDPE technology. LLDPE displays a superior combination of toughness, stiffness, and stress-crack resistance as compared to LDPE. As a result, LDPE has been largely replaced by LLDPE in the tubular film market. Improvement in the physical properties allows the processor to take advantage of LLDPE's good drawdown characteristics, making it possible to produce film having the same thickness but more strength. However, LLDPE poses some processing drawbacks, which prevent it from being successfully processed on conventional LDPE blown-film equipment.

These drawbacks are the result of the unique molecular structure of most LLDPEs, which consists of a narrow molecular weight distribution, short-chain branching, and a low or zero content of long-chain branching. LLDPE melts exhibit a higher

* Present address: Petrobras-Cenpes, Ilha do Fundão, Quadra 7, Rio de Janiero, Brasil.

† To whom correspondence should be addressed.

Journal of Applied Polymer Science, Vol. 58, 2077–2094 (1995)
 CCC 0021-8995/95/112077-18

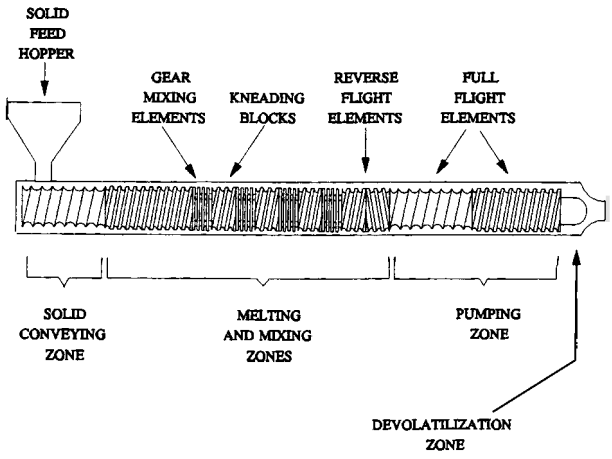

Figure 1 Basic screw configuration.

shear viscosity and a lower elongational viscosity at the usual processing conditions as compared to LDPE with the same melt index. The resulting low melt strength and low strain hardening of LLDPE are reflected in poor bubble stability and in instability at high line rates during film-blowing operations.

New technology in film blowing, such as dual lip air ring technology, lower pressure, spiral dies, grooved barrel feed sections, and high efficiency barrier screws have been developed for improving the processability of LLDPE resins.[1] Also, blends of LDPE and LLDPE have been used widely in the film industry to enhance bubble stability during tubular film extrusion, while taking advantage of the superior physical properties exhibited by the use of LLDPE.[2,3] Another important reason for blending LDPE and LLDPE is to be able to use conventional LDPE film-blowing apparatus without modification.

A reactive extrusion process with low levels of peroxides can offer a practical route for the modification of the extrudability of LLDPEs and there is a growing interest in this method to improve the balance of processability characteristics of polyolefins. However, the following questions are still open: What are the effects of the molecular characteristics of the virgin LLDPE material on the behavior of modified LLDPE? What molecular structure and rheological properties of modified LLDPE are responsible for the modification of processability? Can the reactive extrusion conditions and the method of dispersing the peroxide affect the results?

With the aim of answering these questions, four studies on the reactive processing of LLDPEs were initiated in this research. The present article consists of the first study. This article describes the effects of extrusion process peroxide treatment on the molecular structure of LLDPEs. We are interested particularly in determining whether and how measurements of molecular weight distribution and long-chain branching can be used to interpret effects of reaction conditions on polymer properties. We would also want to determine which measurable properties are the most sensitive and realistic indicators of changes in molecular structure of the reacted LLDPEs.

EXPERIMENTAL

Materials

Two commercial LLDPEs with an MFI of 1.0 were involved in this study. These materials were ethylene–octene copolymers in pellet form and were designated as Resin A and Resin B. These two resins contained a phenolic antioxidant, Irganox 1010™, and were made by the Dowlex process. Molecular weight averages and distributions were similar for the two PEs. 2,5-Dimethyl-2,5 di(*t*-butylperoxy)-hexane (Lupersol 101) was selected as the organic peroxide (provided by Atochem) for the chemical reactions of LLDPE resins under investigation.

Extruder Reactor

The reactive modification of selected resins was carried out on a modular Leistritz twin-screw extruder. A barrel length of 1.2 m was used in all the experiments. The screw diameter was 34 mm, with a length to diameter ratio of 35. Excluding the die, the extruder barrel was divided into 10 zones. Each zone temperature was controlled with electrical resistance heaters and water-jacket cooling. Specific zones were set up as liquid feed ports or as vacuum-devolatilization ports. A microcomputer controlled the extrusion conditions and handled the data acquisition.

The basic screw configuration consisted of a feeding zone, a melting and mixing zone, a pumping zone, and a venting zone (Fig. 1). The feeding section, which had full flight elements, was primarily for conveying solids. The mixing section contained kneading blocks and gear mixing elements. Reverse flight elements were also used to promote good mixing in the extruder. The pumping zone, followed by a venting zone, transported the material toward the die. The pumping zone consisted of full flight elements. In the venting zone, the gases trapped in the melt were extracted. In this work, the twin-screw extruder was used as a corotating intermeshing machine (CRI), labeled System 1.

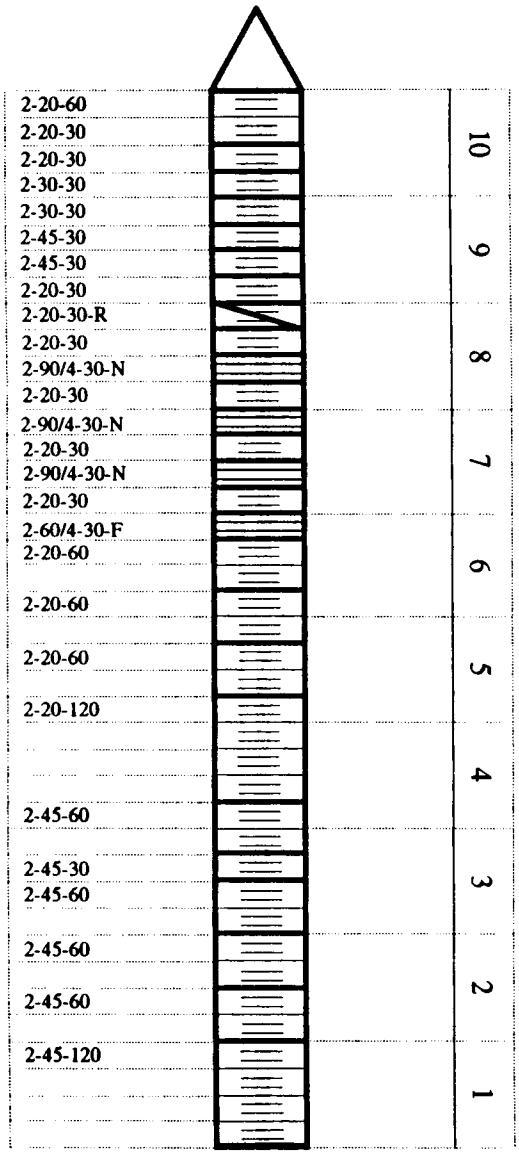

Figure 2 Screw configuration used in System 1–Set 1.

Two screw profiles, labeled Set 1 and Set 2, were used in System 1, as illustrated in Figures 2 and 3. The screw elements are coded according to the nomenclature of the extruder manufacturer [Leistritz]. Equivalent elements may be available from other makers of modular, corotating intermeshing machines; Fig. 4 explains the code.) The feeding zone (1–2) and the pumping zones (9) consisted of full flight elements. This screw configuration facilitated positive conveying characteristics in the extruder. The difference between these two sets was the number of mixing elements employed in the melting and mixing zones of the extruder. Several additional mixing elements were used in Set 2 to provide better dispersion and incorporation of the organic peroxide into the polymer melt. The temperature of the melt was measured at the die. Mechanical energy in the extruder was transformed into heat by frictional and viscous heat generation, and the melt temperature may have often exceeded that of the barrel walls.

Methodology

For the sake of comparison, the selected virgin resins were extruded at the same reaction conditions, but no peroxide was added to the extruder. Figure 5 shows the experimental setup used in System 1–Set 1. The screw speed remained constant at 80 rpm, and the output was controlled at a throughput rate of 40 g/min with a calibrated solids loss-in-weight

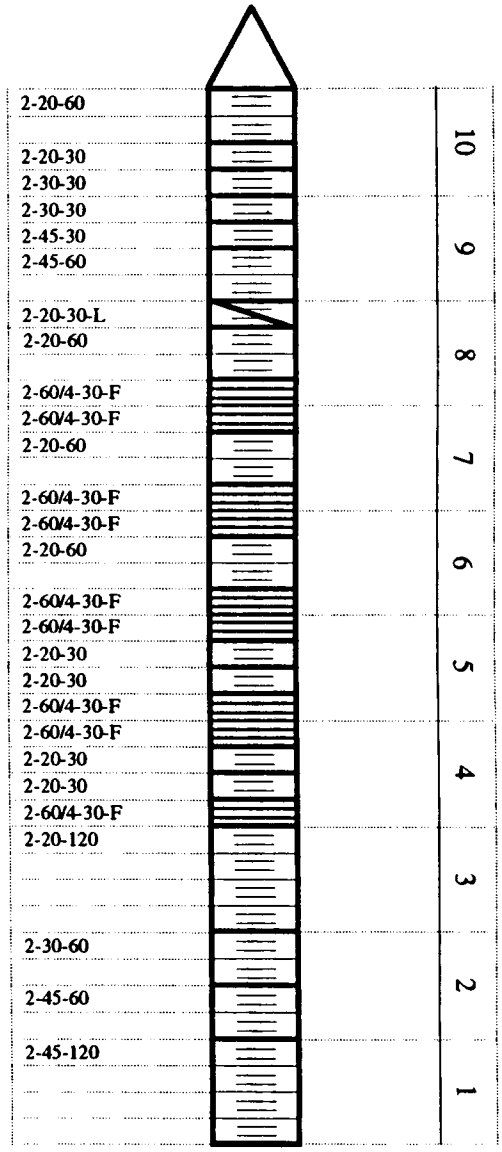

Figure 3 Screw configuration used in System 1–Set 2.

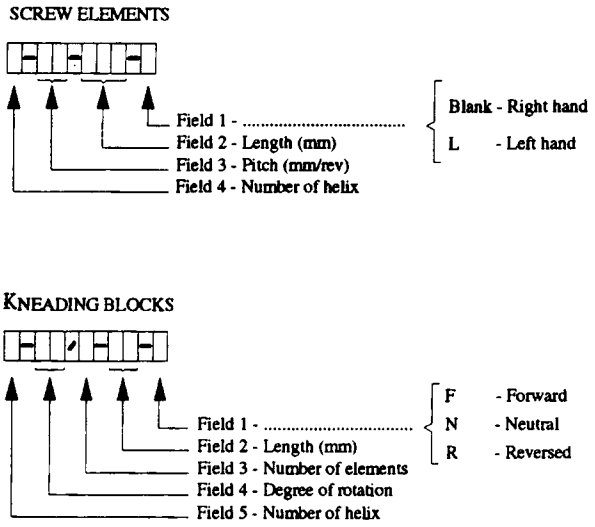

Figure 4 Screw elements and kneading blocks used in corotating configuration.

feeder. The peroxide was previously dissolved in methanol at the appropriate concentration (from about 1.0 to 3.0% [w/w]). The methanol solution was introduced into a feed port in the same zone as the polymer feed, at a controlled rate using a positive displacement liquid pump. A low temperature, ranging from 60 to 100°C, was employed in the first two zones across the extrusion barrel to minimize the chemical reaction of selected resins with the organic peroxide in the conveying zone. In the following zones, a flat temperature profile of 180°C was used across the extrusion barrel.

The melt temperature was measured at the die. During these particular experiments (i.e., System 1–Set 1), the water cooling system was not available. This limited the control of the melt temperature at the die; the melt temperature was approximately 15°C higher than that employed in the mixing and melting zones.

The residence time was measured by adding a colored pellet tracer to the polymer feed and detecting it at the die. Under these conditions, the residence time was approximately 3 min. Devolatilization was accomplished at zone 9 with the aid of a vacuum pump to remove any gaseous products. The extrudate was cooled, dried, and granulated.

It should be noted that a low concentration of peroxide in the range of 0.05–0.15% (w/w) was used in this work to minimize crosslinking of LLDPE under the reaction conditions. Engel,[4] Manley and Qayyum,[5] Dorn,[6] and Kampouris and Andreopoulos[7] suggested that a peroxide concentration of at least 0.2% (w/w) should be used in the industrial crosslinking of PE. This observation was the rationale for the use of a peroxide concentration in the lower range of 0.1% (w/w) in this study, since we want to avoid crosslinking.

This same methodology was used in the reactive modification of selected resins in System 1–Set 2, except that the extrusion barrel temperature in zones 4–10 was maintained at 190°C with the water cooling system (without the latter in System 1–Set 1, the melt temperature at the die was higher than that of the melting and mixing zones). In System 1–Set 2, Resin A was replaced by Resin B, because the latter was more readily available in the quantities needed and had similar processability characteristics to those of Resin A.

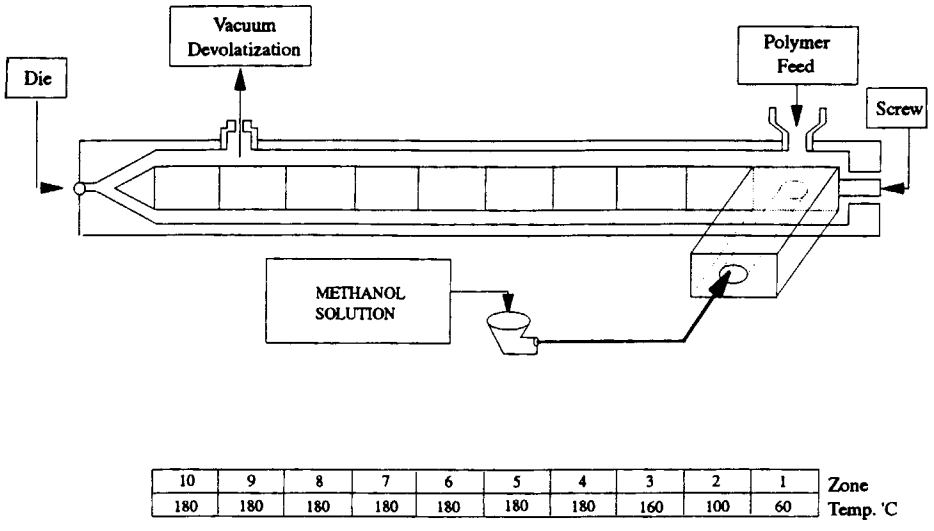

Figure 5 Experimental setup used in System 1–Set 1.

Molecular Characterization

SEC

Molecular weight averages and distributions were measured by a high-temperature size-exclusion chromatograph equipped with a continuous differential refractometer (DRI), low-angle laser light-scattering (LALLS), and differential viscosimeter (DV) detectors. Details of the apparatus and the system of automatic data treatment were reported elsewhere.[8] The apparatus was run at 145°C. 1,2,4-Trichlorobenzene (TCB) containing 0.1% Irganox 1010™ antioxidant was used as the solvent for the system and for sample preparation. The solvent flow rate was 1 mL/min. Samples of PE solutions in TCB at 1–2 mg/mL were injected into the SEC unit at 145°C. Sample dissolution was accomplished by rotating the sample vials for 24–72 h at 160°C. This procedure was suggested by Rudin et al.[9] to eliminate the PE supermolecular aggregates that tend to persist at 145°C in TCB.

A mixed-bed column packed with polystyrene gel was calibrated with narrow-distribution polystyrene standards. The molecular weight averages of PE resins were calculated using the universal calibration procedure and Mark–Houwink constants reported by Rudin and co-workers.[10,11] In this work, reported M_z values of selected resins were calculated from SEC–LALLS data. Kulin and co-workers[12] noted that the high molecular weight fraction of polymer samples was detected better by the LALLS detector, while the DRI (concentration detector) was less sensitive. Pang and Rudin[13] reported similar results using the system mentioned previously. M_w and M_n values were calculated here from SEC–DV data. The values listed for each resin under investigation were an average of the data of three different sample solutions. Long-chain branching was assessed as a function of molecular weight, using the SEC method described elsewhere.[14]

DSC

The thermal behavior of virgin resins and reactive extrusion products was characterized by DSC on a Perkin-Elmer DSC-4 differential scanning calorimeter equipped with thermal analysis data acquisition software. All samples were pressed at 190°C for 10 min under 20,000 lb force and then cooled at 10°C/h in a controlled oven. This annealing procedure was used to maintain a uniform thermal history between the samples.[15] Polymer samples of 6–10 mg were encapsulated in standard aluminum pans. The endotherms were measured at a heating rate of 10°C/min over a range of 40–170°C. An indium standard was used to calibrate the temperature scale and enthalpy of melting. The reproducibility of the DSC curve shape was checked by running replicate annealed samples of selected modified resins.

Table II C—C Double Bonds in Resins A and B

Resin	Terminal Unsaturations[a]	Trans Unsaturations[a]
A	0.55	0.14
B	0.56	0.14

[a] Concentrations are given in unsaturations per 1000 carbons.

TREF

Temperature rising elution fractionation (TREF) profiles of selected resins were generated using an instrument built at the University of Waterloo. Samples were dissolved at an approximate concentration of 7 mg/mL in 1,2,4-trichlorobenzene containing 0.1% Irganox 1010™ as the antioxidant. Details of the system and data acquisition are reported by Karbashewski and co-workers.[16] The purpose of using this technique was to compare the TREF profile to the DSC curve shape generated by thermal analysis, as well as to investigate the short branching distribution of selected samples.

Gel Content

The gel content of samples under investigation was measured by a solvent extraction technique. Bremner[17] suggested that this method could provide consistent

Table I Molecular Characteristics of LLDPEs A and B

	Molecular Weight Averages					
	M_z (10^{-3})	M_w (10^{-3})	M_n (10^{-3})	M_w/M_n	Short Chain Branches[a]	ΔH_{melt} (J/g)
A	370	73	24	3.0	15	85
B	380	77	25	3.1	14	84

[a] Branch content is given per 1000 backbone carbons.

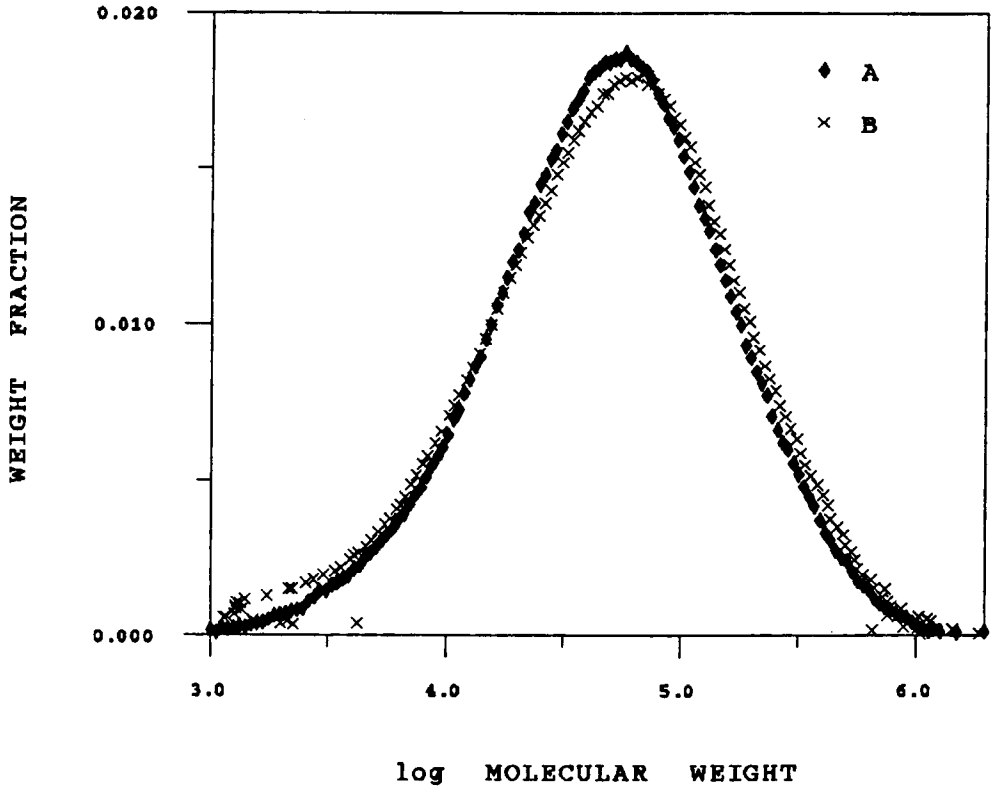

Figure 6 Molecular weight distributions of Resins A and B, from SEC using a continuous viscometer.

results, although its accuracy is still questionable. Samples were placed in 120 mesh stainless-steel baskets and immersed in boiling xylene. Extractions were run for 24 h. The samples, after removal from the boiling solvent, were dried at 60°C under vacuum to remove any residual xylene and weighed to determine the percentage of gel content.

^{13}C-NMR for Branch Content

In the field of ^{13}C-NMR analysis of copolymers, ethylene-1-olefin copolymers have been studied in relation to the analysis of the various kinds of branching structures that exist in the LLDPE. Ray et al.[18] and Hsieh and Randall[19] described the detailed assignments of ^{13}C-NMR signals of ethylene-1-butene copolymers. Randall[20] provided the spectra for copolymers with low comonomer fraction, leading to isolated units. Branches shorter than six carbon atoms could be clearly ascertained from their ^{13}C-NMR spectrum. However, branches of six carbons in length could not be differentiated from longer-chain branches.[21]

Measurements of branching in virgin resins and reactive extrusion products were made on a Bruker AC 300 MHz spectrometer at 75.43 MHz. The spectra were recorded using an inverse-gated pulse sequence and a 90° pulse width. A 12 s relaxation delay was used between the pulses. Base-line resolution was achieved in approximately 2000 scans. The operating temperature was 120°C, while the sample preparation was accomplished by swelling the polymer, with a concentration of approximately 40% by weight in 1,2,4-trichlorobenzene, at 150°C for 1 h. The content of the hexyl branches in ethylene–octene copolymers under investigation was calculated from the relative peak areas of CH_2 at 29.99 ppm to that of the 3B6 (third carbon from the branch end on a six-carbon branch) carbon at 32.2 ppm.[22,23] The number of ethyl branches in ethylene–butene copolymers under investigation was measured from the relative peak area of the CH_2 peak at 29.99 ppm to that of the 1B2 (first carbon from the end of a ethyl branch) carbon at 11.2 ppm. Peak areas were measured by planimetry on expanded scale plots. (Branching is reported as the number of branches per 1000 backbone carbons.)

FTIR Analysis for Vinyl Unsaturation

The vinyl unsaturation data of virgin resins and reactive extrusion products was measured using a Ni-

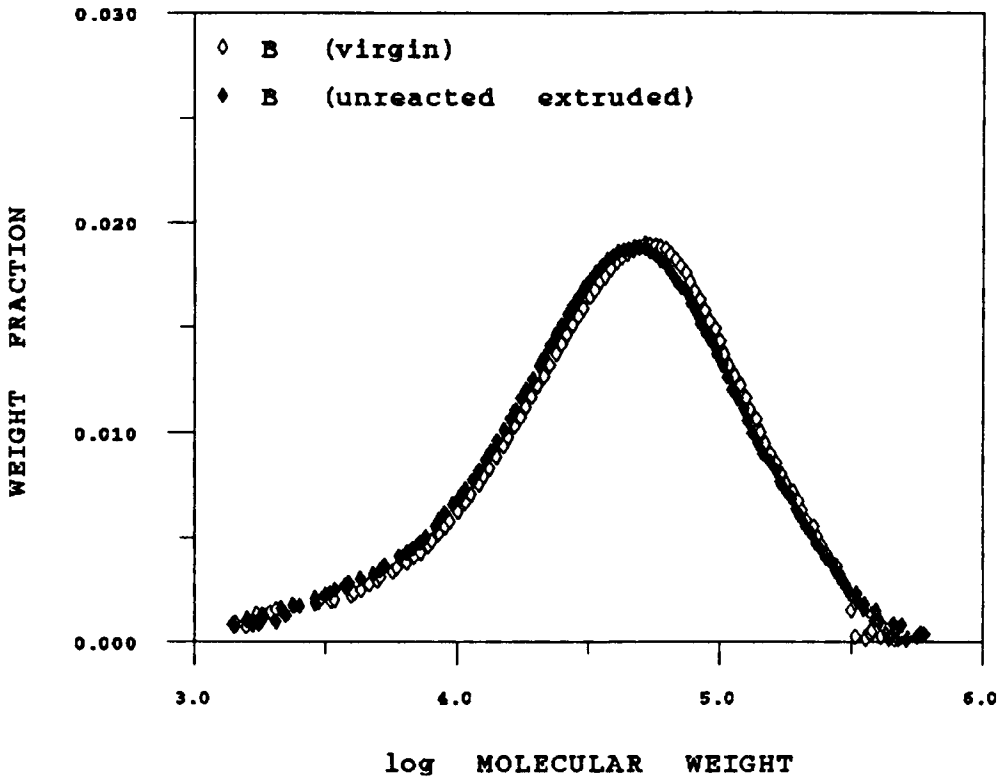

Figure 7 Molecular weight distributions of Resin B, virgin and unreacted extruded, from SEC using a continuous viscometer.

colet Model 520 FTIR at 1 cm^{-1} resolution. Samples were pressed at 190°C for 10 min; then, thin films of approximately 0.3 mm were used for vinyl unsaturation content measurements. Peaks from absorbance spectra were assigned to out-of-plane C—H bends, associated to terminal unsaturations (908 cm^{-1}), *trans*-vinyls (964 cm^{-1}), and pendant vinyls (888 cm^{-1}). The pendant vinyls were not reported, because the band at 888 cm^{-1} assigned to this type of unsaturation was obscured by the peak at 850 cm^{-1} assigned to the terminal methyl of a branch of C_4 or longer.[24] The unsaturation content (reported as C—C double bonds per 1000 carbon atoms) was calculated by the measured peak height absorbance of the respective type of unsaturation and the extinction coefficient reported by Haslam et al.[24] The extinction coefficient was required to convert the absorbance to number of double bonds per 1000 carbon atoms.

RESULTS

Molecular Characterization

Tables I and II list some of the molecular characteristics pertaining to Resins A and B. The molecular weight distributions of these two resins are illustrated in Figure 6. Resin B has the slightly broader molecular weight distribution. Resin A has similar branching and unsaturation characteristics to Resin B; therefore, it is expected that these two resins would behave quite similarly upon peroxide modification. In this study, samples are assigned two code numbers, the first corresponding to the resin under investigation, and the second, in brackets, to the peroxide concentration.

Figure 7 shows the molecular weight distribution overlays of virgin and unreacted, extruded Resin B measured from SEC using a continuous viscometer.

Table III Molecular Weight Averages of LLDPE A After Reactive Extrusion in System 1–Set 1

Resin[a]	M_w (10^{-3})	M_n (10^{-3})	M_w/M_n	M_z (10^{-3})
A	73	24	3.0	370
A [0.05]	93	24	3.9	401
A [0.10]	96	24	4.0	408
A [0.15]	102	24	4.3	433

[a] Term in [ ] refers to peroxide concentration during extrusion.

Table IV Molecular Weight Averages of LLDPE B After Reactive Extrusion in System 1–Set 2

Resin	M_w (10^{-3})	M_n (10^{-3})	M_w/M_n	M_z (10^{-3})
B	77	25	3.1	380
B [0.05]	84	27	3.1	417
B [0.10]	95	28	3.3	466
B [0.15]	97	29	3.3	484

Table V Effect of Reactive Extrusion in System 1–Set 1 on Molecular Weight Distribution of LLDPE A

Resin	Molecular Weight Above 10^5 (Weight Fraction) (Universal Calibration)	Molecular Weight Above 10^5 (Weight Fraction) (Continuous Viscometer)
A	22	22
A [0.05]	28	30
A [0.10]	31	31
A [0.15]	33	32

These distribution curves show no appreciable differences between the two samples. Therefore, the extrusion process itself can be eliminated as a variable in the rationalization of observed molecular structure differences of peroxide-modified samples compared to that of virgin resins. It is known that oxidation, shear, and thermally induced reactions take place in the degradation process of PE,[25] but these are not evidently significant in the extrusion conditions process used here. Similar results were observed for Resin A.

Table III lists the molecular weight data for Resin A before and after peroxide reaction in System 1–Set 1. M_n and M_w were determined from continuous viscometer data, and M_z, from LALLS data, as those were deemed to yield the best representation of the molecular weight characteristics of the resins under investigation. The weight-average molecular weight, M_w, increases as the peroxide concentration is increased. A more significant effect is revealed by the M_z values. These results are expected, since the M_z average is more suitable to estimate the high molecular weight material in a polymer sample. A similar trend (Table IV) is shown for the reactive extrusion products generated in System 1–Set 2. In addition, the peroxide-modified samples have a broader molecular weight distribution compared to

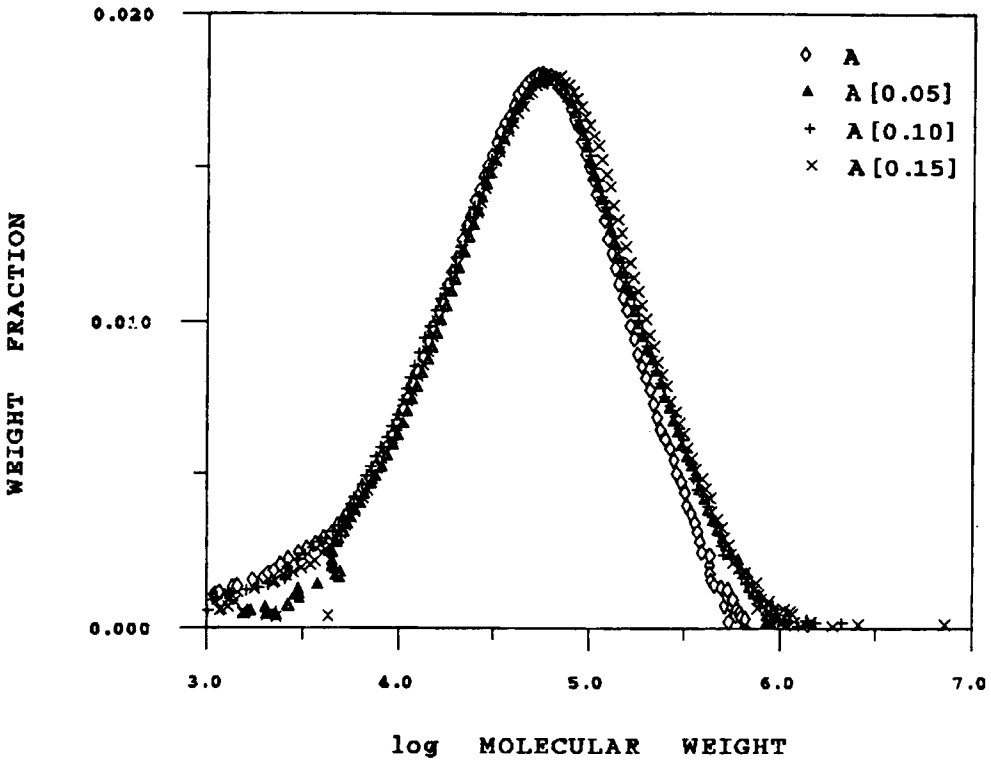

Figure 8 Molecular weight distributions of sample set A[n] from SEC using a continuous viscometer.

that of unreacted resins, indicated by higher M_w/M_n values for the former samples.

Figure 8 shows a plot of the normalized concentration as a function of log molecular weight of resins generated in System 1–Set 1, as determined from SEC using a continuous viscometer. The molecular weight distributions of the peroxide-reacted samples are all shifted to the high molecular weight end, compared to unreacted extruded Resin A, but the effects of the different peroxide concentrations in the range studied are not readily apparent in such plots.

The effect of the peroxide concentration on the molecular weight distribution of peroxide-modified samples (Table V) generated in System 1–Set 1 is better demonstrated by comparing the weight fraction of the normalized distribution curve at the highest molecular weight end (above 10^5) of Resin A to that of reactive extrusion products. As expected, the weight fraction of the highest molecular weight end ($>10^5$) increases as the peroxide concentration is increased. These results summarize the polymer chain extension that takes place in the presence of peroxide-derived free radicals during the reactive process.

It has been noted that the molecular weight distribution curves of Resin A[0.10] and Resin A[0.15] generated in System 1–Set 1 (Fig. 8) are only slightly different. For the reactive extrusion products generated in System 1–Set 2 (Fig. 9), the changes in the distribution curves upon peroxide modification are more significant than are those generated in System 1–Set 1. In addition, the weight fraction of the high molecular weight end measurements (compare Table V to Table VI) indicates a similar trend. The differences between Set 1 and Set 2 reflect the better temperature control and mixing in Set 2. However, it is still noteworthy that only slight differences are shown between the molecular weight distributions

Table VI Effect of Reactive Extrusion in System 1–Set 2 on Molecular Weight Distribution of LLDPE B

Resin	Molecular Weight Above 10^5 (Weight Fraction) (Universal Calibration)	Molecular Weight Above 10^5 (Weight Fraction) (Continuous Viscometer)
B	22	22
B [0.05]	30	30
B [0.10]	34	33
B [0.15]	35	34

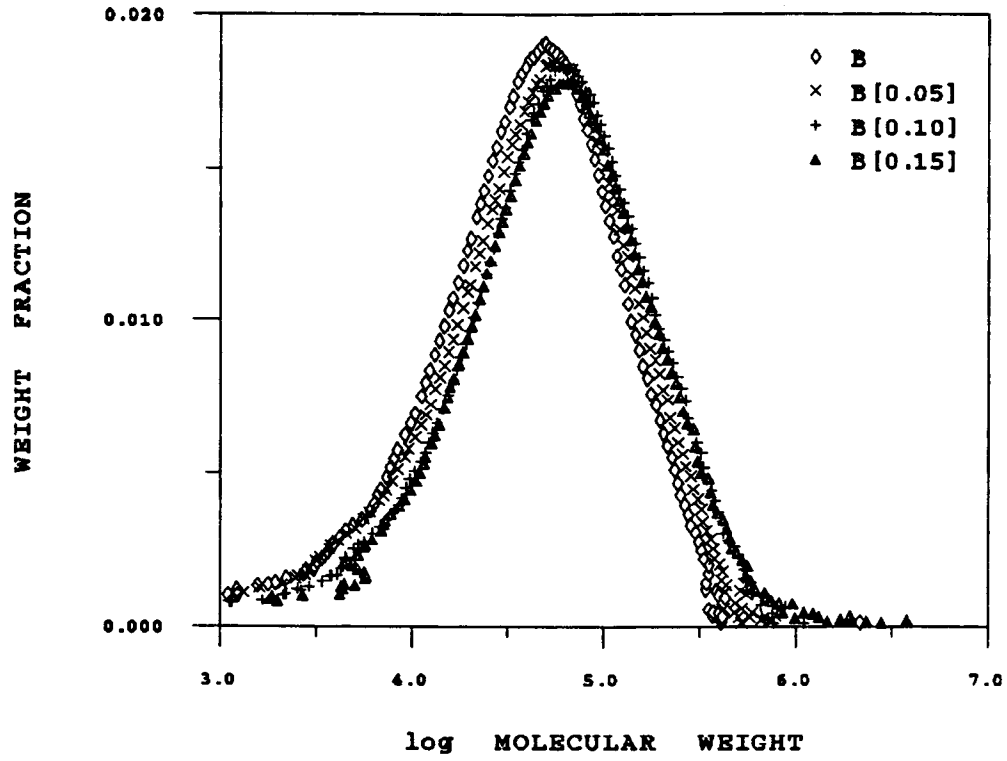

Figure 9 Molecular weight distributions of sample set B[n] generated in System 1–Set 2 from SEC using a continuous viscometer.

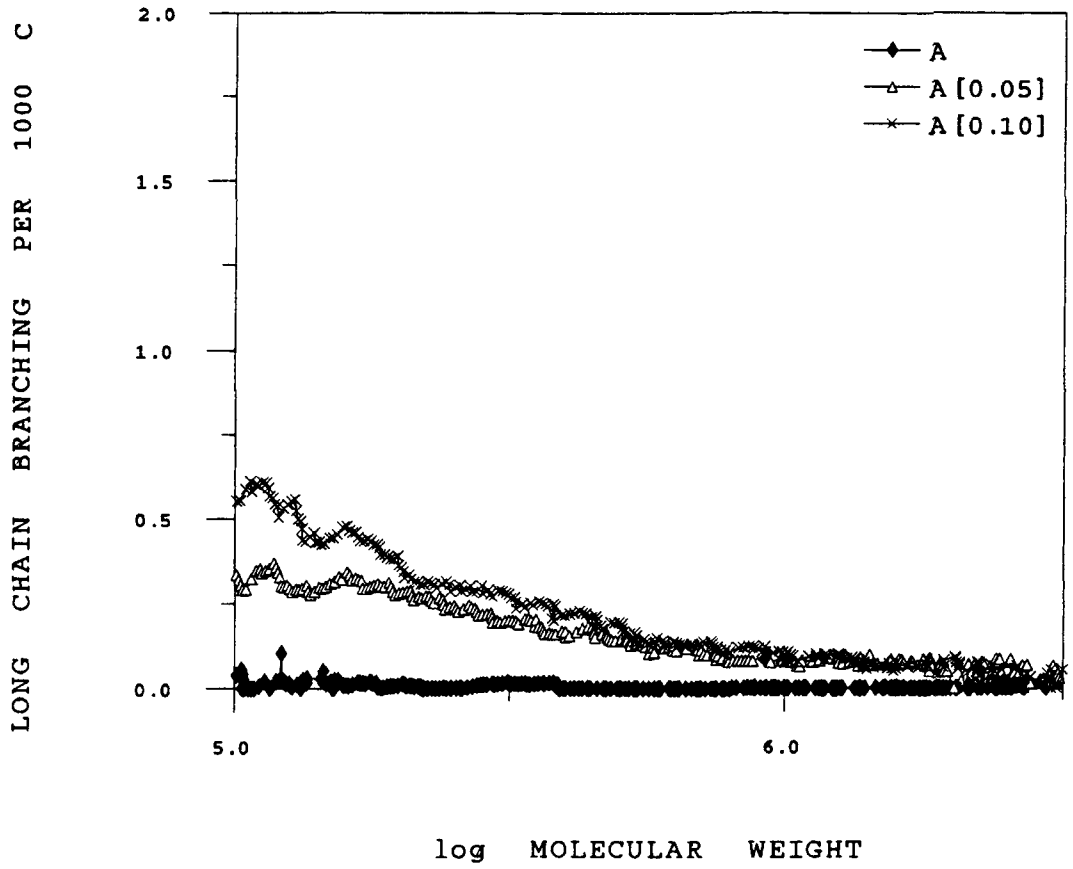

Figure 10 Tetrafunctional long-chain branch frequency as a function of molecular weight of sample set A[n] generated in System 1–Set 1.

of Resin B[0.10] and of Resin B[0.15] (Fig. 9 and Table VI).

Molecular weight distributions determined by SEC analyses can be used to measure long-chain branching (LCB) in polyolefins as a function of molecular weight.[14] This procedure compares the molecular weights of linear and branched polymers which have equivalent hydrodynamic volumes. The long-branch frequency is estimated by invoking a particular model to relate the radius of gyration and molecular weight. This model, due to Zimm and Stockmayer,[26] assumes randomly branched polymers with trifunctional or tetrafunctional branch points. It also assumes the existence of Theta solutions. The experimental parameters, g', are values of the ratio of the hydrodynamic volumes of linear and branched species with the same molecular weights. To proceed further, to obtain the corresponding ratio of radii of gyration, g, one must assume the magnitude of an exponent which lies between 0.5 and 1.5:

$$g' = g^k \qquad (1)$$

(Details of the assumptions and physical relations are summarized in Ref. 14.) Once g has been calculated, the long-branching concentration can be estimated, using the appropriate Zimm–Stockmayer model.

It should be noted that the branches in LLDPEs are not registered in SEC analyses, at least at the branch levels and lengths in current commercial products. In such products, the minimum branch length that can be perceived as "long" in such SEC analyses is $> C_6$ and $\leq C_{12}$.[27] Despite the serious assumptions involved, SEC analyses of long branches in PEs are consistent with ^{13}C-NMR analyses in which model assumptions are not involved.[14,28]

Here, we used Bersted's approximations[29] to solve the Zimm–Stockmayer relations. The results are in terms of number of long branches, with unspecified lengths, per 1000 carbons. The exponent k, in eq. (1), was taken to be 0.7. Choice of a lower value (i.e., 0.5) would increase the estimated long-branch frequency. It appears not to be possible to select the exponent a priori.[27]

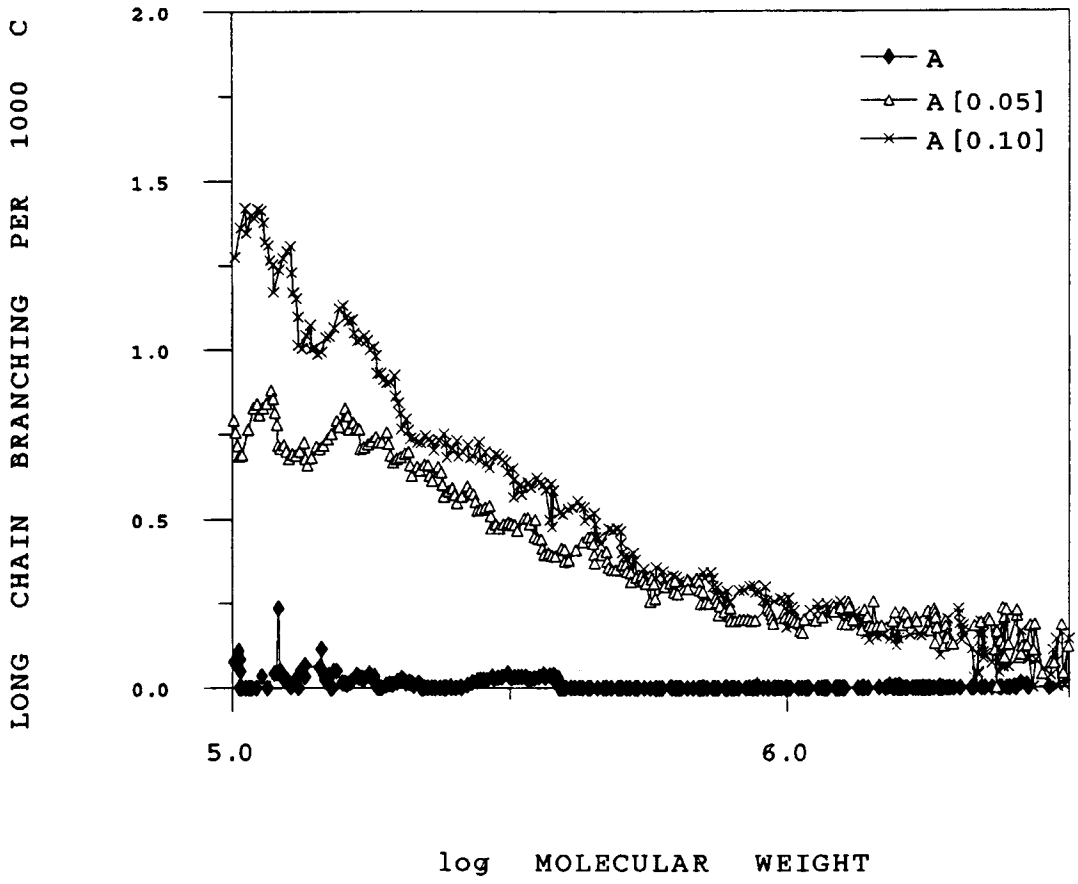

Figure 11 Trifunctional long-branch frequency as a function of molecular weight in sample set A[n] generated in System 1–Set 1.

Figure 10 illustrates the long-branch frequency of LLDPE A before and after peroxide treatment, as a function of molecular weight, using the SEC analyses with continuous viscometer analyses. In this case, the estimates were based on the Zimm–Stockmayer model with tetrafunctional branch points. Figure 11 shows the results of parallel calculations assuming a Zimm–Stockmayer model with trifunctional branch points. These results were calculated from the raw SEC elution volume—molecular weight results without data smoothing—hence, the noise in the curves. As expected, the level of LCB in the virgin Resin A is undetectable over the entire observed molecular weight range. The level of LCB increases with increasing peroxide concentration. A similar trend is shown for the reactive extrusion products generated in System 1–Set 2 (Fig. 12). It is interesting that the increase of the level of LCB is slightly more significant for the peroxide-modified resins generated in the System 1–Set 2 as compared to those prepared in System 1–Set 1. This reflects the tighter temperature control and better mixing in Set 2 and shows that fairly minor process changes can produce significant differences in the properties of the modified PEs.

Table VII lists the results of ^{13}C-NMR analyses of Resins A and B that have been extrusion-reacted with 0.05% peroxide. Samples that had been treated with higher peroxide levels resisted such analyses because of line broadening, possibly from the presence of microgel which was otherwise not detectable. Long-branch content is indicated by the differences between the branch contents of the untreated and reacted polymers. As mentioned earlier, this technique cannot distinguish reliably between C_6 and longer branches. In this case, the mean long branch content of sample A [0.05] is 2 branches/1000 backbone carbons, while that of sample B [0.05] is 3/1000 carbons. Reference here is to long branches at trifunctional branch points. The ^{13}C-NMR analyses did not detect any tetrafunctional branch points in these materials.

The ^{13}C-NMR and SEC long-branch measurements are mutually consistent, in line with experi-

ence with other PEs.[14,28] The SEC branch content calculations are lower than those from NMR, again in line with general experience. The former could be increased by choosing the exponent in eq. (1) to be 0.5, instead of 0.7, as was done here. The lack of exact coincidence may also reflect the fact that the Zimm–Stockmayer model is not strictly applicable to these polymers in good solvents. In any event, it is clear that the SEC technique produces estimates of peroxide-induced long-branch content that are reasonably close to those of NMR analyses that generate data which are independent of the assumptions involved in the SEC method.

In the present case, the mean long-branch content in the modified polymers is about 0.75 per 1000 carbons, from Figures 11 and 12. This corresponds to 3.9 long branches per weight average molecule ($\bar{M}_w$ = 73,000) or 1.3 branches per number-average molecule (M_n = 24,000). The long-branch contents generated by the processes used here are of the same order of magnitude as in LDPEs.[12] However, the effects of this branch frequency can be detected with more sensitivity by rheological measurements. These latter data will be discussed in the subsequent article.

Table VII Hexyl and Longer Branches in Untreated and Reacted LLDPEs

Resin	Hexyl or Longer Branches (per 1000 Backbone Carbons)
A	14
A [0.05]	16
B	15
B [0.05]	18

The SEC and NMR long-branch measurements provide further information about the free-radical reactions involved here. Details are postponed until after consideration of the concurrent changes in carbon–carbon unsaturation.

The role of terminal unsaturations in increasing crosslinking efficiency, or coupling reactions, has been studied previously,[30,31] although the exact mechanism is not always agreed. Bremner and co-

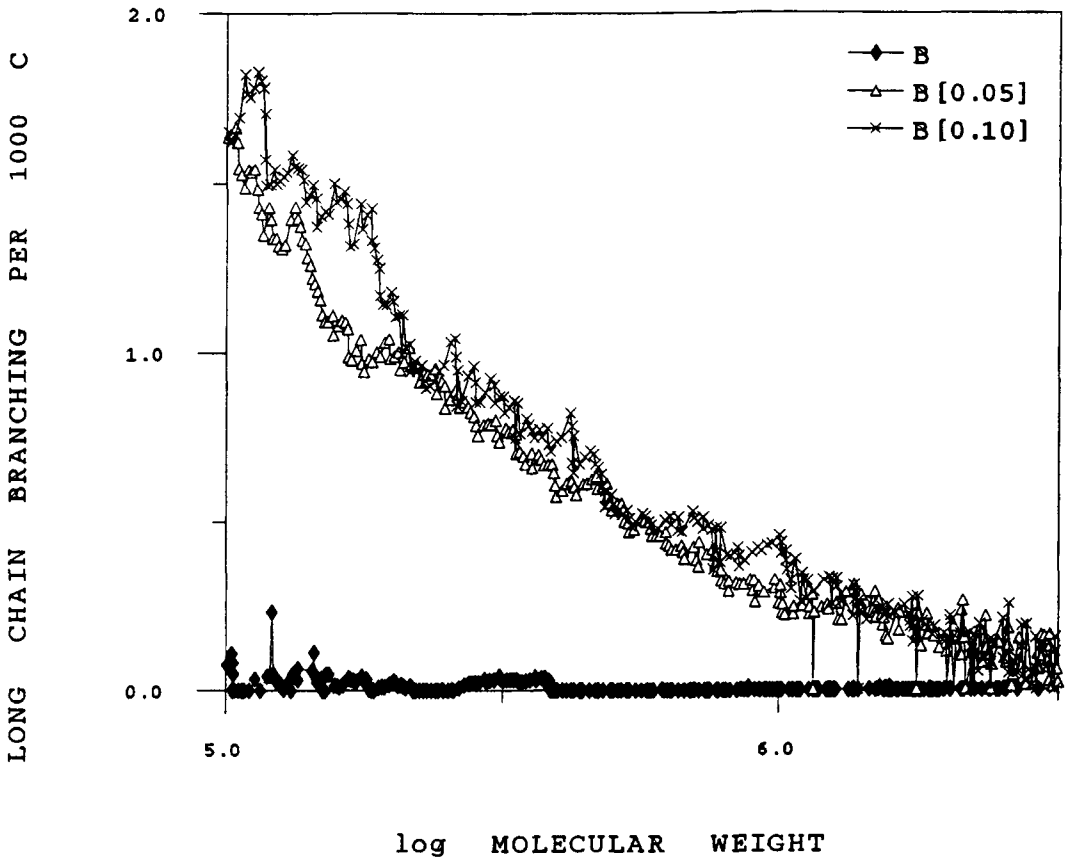

Figure 12 Trifunctional long-chain branch frequency as a function of molecular weight of sample set B[n] generated in System 1–Set 2.

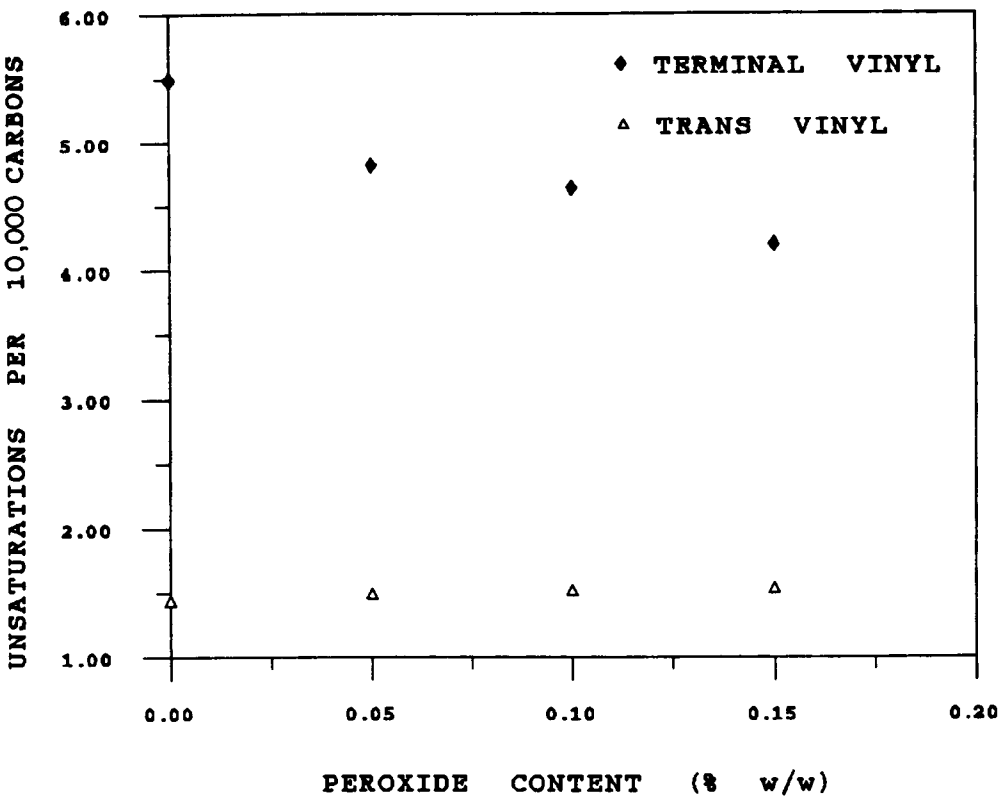

Figure 13 Vinyl unsaturation contents of sample set A[n] generated in System 1–Set 1.

workers[32,33] reported the major contributing reactions of terminal vinyls in a free-radical scheme that accounts for the changes in vinyl group concentrations in PE.

The significant reduction in the amount of terminal unsaturations in peroxide-modified resins generated in System 1–Set 1 (Fig. 13) and in System 1–Set 2 (Fig. 14), compared to that of Resins A and B, is in accord with the mechanism proposed by Bremner and Rudin.[32] These conclusions agree with the work done by Hendra and co-workers[30]; chain-extension reactions account for a decrease in the amount of terminal vinyls upon peroxide reaction. Allylic radicals are an intermediate species in chain-coupling reactions involved in peroxide modification of LLDPE yielding *trans* or *cis* unsaturations. This is demonstrated by a significant shift in the molecular weight distribution curves of Resin A[0.05] (Fig. 8) and Resin B[0.05] (Fig. 9) toward the high molecular weight end compared to unreacted extruded Resin A. Simultaneously, the number of *trans* unsaturations tends to increase slightly with peroxide concentration (Figs. 13 and 14).

Although many reactions are conceivably involved in the chain of events that can be initiated by peroxide-derived free radicals,[30,32] the major reactions that are of interest here are apparently those listed in Figure 15. The most stable radicals that can be generated as a result of hydrogen abstraction by peroxide-derived radicals or their descendants are those produced at carbons allylic to double bonds. The allylic radicals from terminal double bonds are particularly important in this regard because addition of other radicals is facilitated compared to allylic positions internal to the polymer chain. Long-branch formation is apparently primarily by coupling of secondary radicals with such terminal allylic radicals. Such reactions cause a decrease in terminal unsaturation, as observed, and an increase in internal unsaturation. Interconnection of such long branches would lead to crosslinking.

There is no experimental evidence of addition of tertiary radicals to terminal allylic radical sites to produce long branches at quaternary carbon branch points. Generation of tertiary radicals by hydrogen abstraction is energetically favored over production of secondary radicals, but the difference in bond energies of tertiary and secondary C—H linkages is slight (93 vs. 95 kcal/mol, as compared to 86 kcal/mol for allylic hydrogens)[34] and methylene hydrogens outnumber methine hydrogens in these polymers by about 130/1 (Table I). It is not surprising,

then, that the predominant reaction involved in long-chain branching is addition of secondary radicals on the LLDPE backbone to allylic radicals at the molecules ends.

Figures 11 and 12 indicate a decreasing long-branch level with increasing molecular weight of reactively extruded products. Several reasons may be advanced for these observations: Noise is unlikely to be a factor since these effects are manifested particularly at both the high and low molecular weight tails of the distributions.[35] It is possible that at least some of the apparent increase in long-chain branching in the low molecular region may reflect a problem in "universal calibration" of the SEC apparatus and, consequently, in estimating molecular weights of linear polymer with hydrodynamic volumes equivalent to those of lower molecular weight branched polymers.[36] The most plausible explanation is, however, that the efforts observed are real. The untreated polymers had an M_n of 24,000 and contain 0.54 terminal vinyl groups per 1000 carbons. This is equivalent to 0.9 terminal vinyls per number-average molecule (taking the methylene formula weight of 14 for each carbon). The catalyst composition and polymerization mechanism of the Dowlex process has not been published, to the author's knowledge, but these results imply a molecular growth reaction that yields terminal carbon–carbon double bonds. Since the chain-extension process appears to be end-linking and since terminal vinyls dominate this reaction, the formation of a single long-branch per molecule results in a higher concentration of such branches (expressed per 1000 carbons) the smaller the initial molecule.

Peroxide-induced long-branch formation is apparently similar mechanistically to radiation-induced modifications of the PE molecular structure. Randall and co-workers[37] employed ^{13}C-NMR analyses to study the effects of radiation on a solid, linear PE. As in our study, the process was limited to radiation doses less than the gel dose. The important finding of this study was that long-chain Y branches were formed in preference to crosslinks (H branches). The former were suggested to be formed by addition of a secondary radical to a terminal vinyl, while the latter result from mutual termination of two secondary radicals. An alternative to the suggested mechanism for the Y branch (i.e., tertiary branch points) formation is termination of a secondary radical by an allylic end radical. Experimental evidence is insufficient to distinguish between these possibilities.

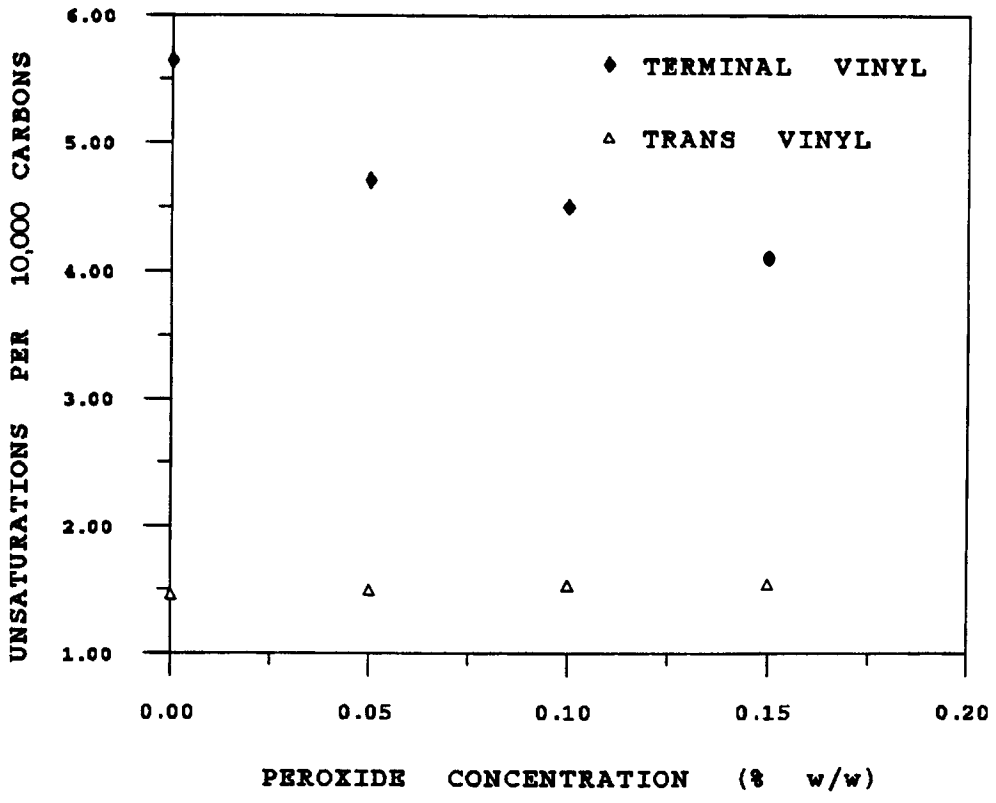

Figure 14 Vinyl unsaturation contents of sample set B[n] generated in System 1–Set 2.

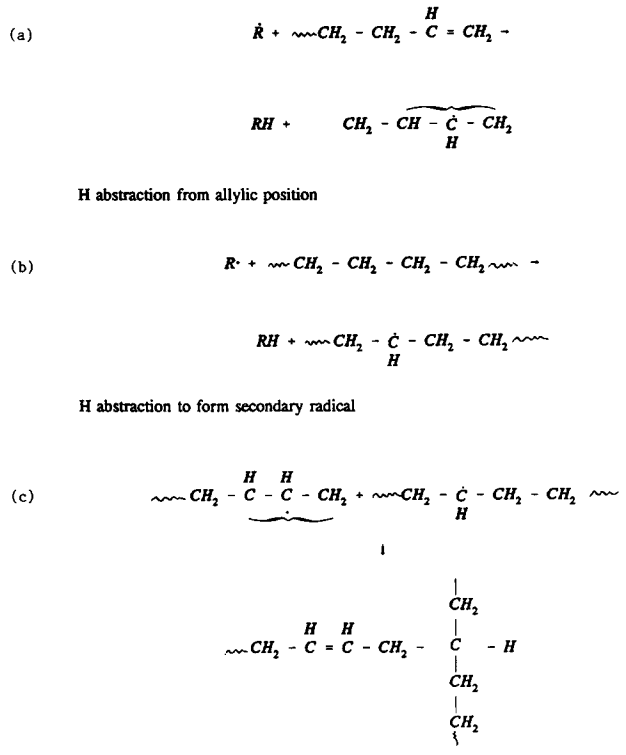

Figure 15 Important reactions in long-branch formation.

In later studies, Horii and co-workers[38,39] irradiated low molecular weight linear PE species in the molten state. Their results showed that more H links than Y links were produced. However, the unsaturation characteristics of their polymers were not reported. The apparent discrepancy is possibly due to differing terminal vinyl contents in the two polymers used in the two studies. The exclusive production of Y-type branches noted in this research may not persist with LLDPE resins that have much lower unsaturation levels.

A preliminary qualitative inspection of peroxide-modified sample tapes generated on a single-screw extruder indicated no appreciable presence of microgel in all selected resins, as examined using an optical microscope. These findings revealed good dispersion and homogeneity in reaction products generated in System 1–Set 1 and in System 1–Set 2. In addition, the analysis of gel content indicated that the amount of insoluble material is negligible in all reactive extrusion products generated in System 1. Note, however, that line-broadening in the ^{13}C-NMR spectra of reacted products gave contrary indications.

It is known that in crosslinking PE with organic peroxides the extrusion process conditions must be controlled, since peroxide incorporation and the processing of the peroxide mixture should take place without premature crosslinking (scorching). The absence of microgel as indicated by the clear films of all extrudates demonstrates that the extrusion process conditions used in System 1–Set 1 and in System 1–Set 2, as well as the method of dispersing

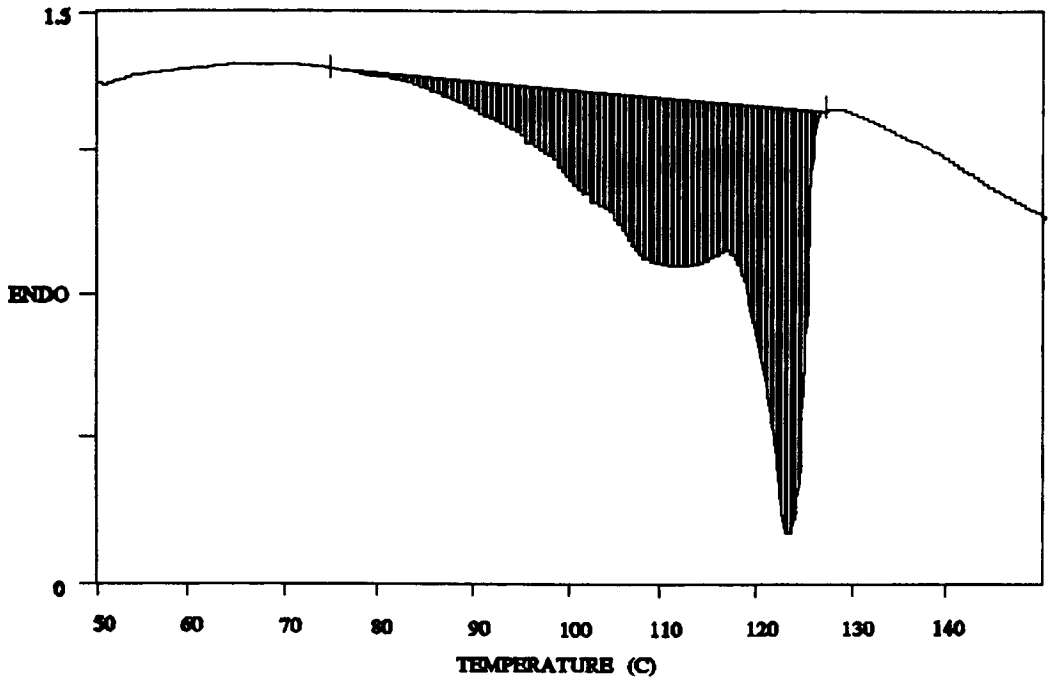

Figure 16 DSC endotherm of Resin B.

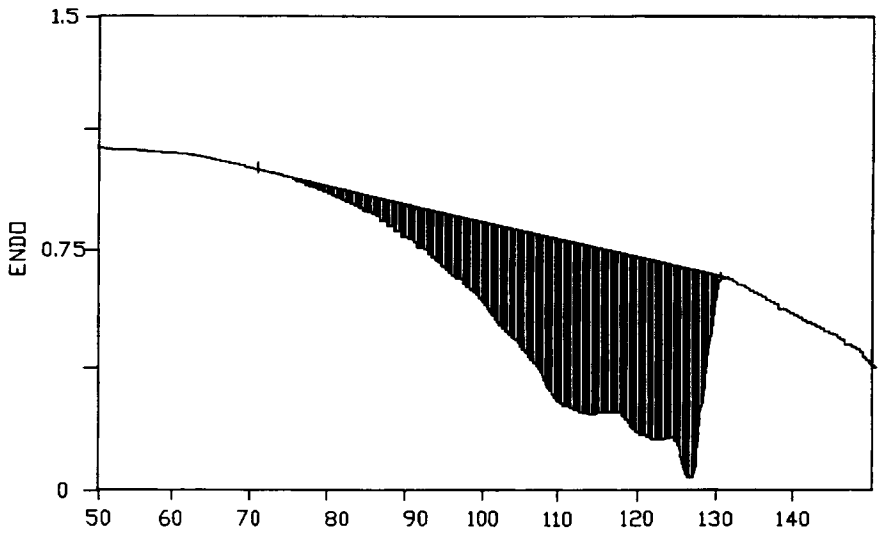

Figure 17 DSC endotherm of Resin B[0.05] generated in System 1–Set 2.

the peroxide, were reasonably successful in generating homogeneous products. While these practical evaluations indicated the absence of microgel, there was indirect evidence of its presence from the line broadening in ^{13}C-NMR spectra. Such NMR analyses are indicated to be a very sensitive, if very exotic, method to detect microgel in products made by reactive extrusion with peroxides.

The changes in the thermal behavior for Resins B, B[0.05], and B[0.15] upon peroxide modification are demonstrated in Figures 16–18. The intensity of the peak pertaining to the linear polymer fraction decreases with increasing peroxide concentration, while the peak at the lower temperature pertaining to the branched materials becomes broader. In general, branching reactions in a polyolefin reduce its crystallinity. It seems that even a low concentration of the peroxide added during the extrusion process of LLDPE in consideration is reflected in an easily detectable increase of chain irregularities. The shape of the branching distributions of Resins B and B[0.15], generated by TREF analysis (Fig. 19), are in accordance with the DSC endotherm curve shape (Figs. 16–18). As expected, the reactive extrusion product, Resin B[0.15], exhibiting the broadest TREF elution profile at the lowest temperature, was

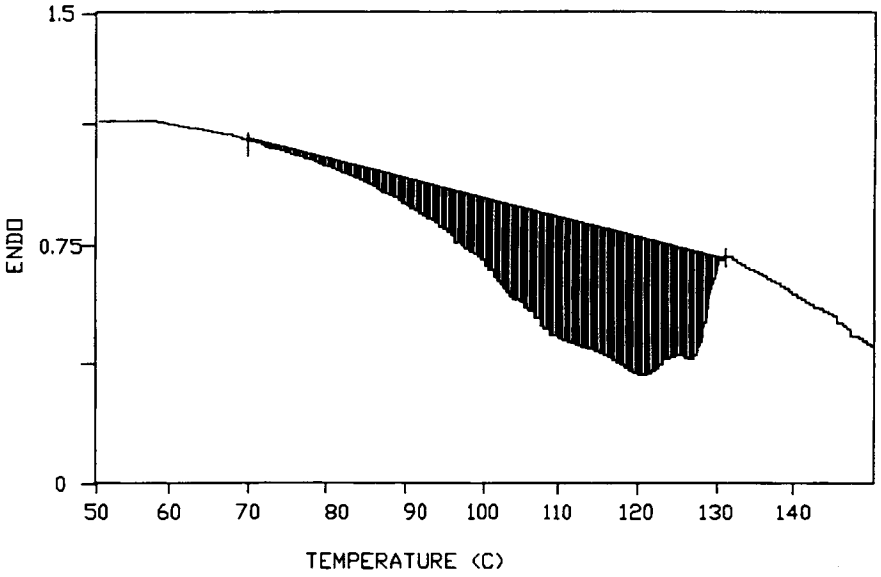

Figure 18 DSC endotherm of Resin B[0.15] generated in System 1–Set 2.

determined to have the broadest melt temperature range in the DSC analysis.

The melting enthalpy ΔH_{melt} values (Table VIII) also show some interesting correlations to the DSC endotherms and TREF profile. As expected, ΔH_{melt} decreases as the peroxide concentration increases, indicating that the chain irregularities in a polymer chain increase upon peroxide treatment. In addition, the relative area of the DSC peaks at the highest melt temperature (pertaining to the linear material) compared to that of the lowest melt temperature (pertaining to the branched fraction) decreases as the peroxide concentration increases. Similar trends are shown as determined by TREF analyses.

Table VIII ΔH_{melt} of Reacted Polymers

Resin	ΔH (J/g)	Temperature (Onset, °C)	Temperature (Melt, °C)	Area %[a] (TREF)
B	84	117	123	18
B [0.05]	79	114	121.7	—
B [0.15]	78	92	114.7	15

[a] Area of higher melting to lower melting peak.

CONCLUSIONS

Careful control of the process for admixing peroxide and reactive extrusion can produce products that are practically gel-free. Changes in molecular structure that are observed include the expected increase in the high molecular weight portion of the distribution with increased peroxide content. The creation of branches during reactive extrusion was evident particularly by changes in DSC and TREF analyses curves. The variations in long-branch content at low peroxide levels are measured to some extent by ^{13}C-NMR techniques. This method is limited by line-broadening effects which can result from incorporation of paramagnetic impurities (e.g., steel from the extruder) or from crosslinking at higher peroxide levels. Molecular weight augmentation was primarily by end-linking of terminal vinyls or allylic radicals at the chain ends with secondary radicals on other molecules. Long branches originated from tertiary branch points. SEC analyses show that the number of long branches per molecule is inversely proportional to the size of the initial, unreacted LLDPE molecule as would be expected if the termination reaction in the LLDPE polymerization generated unsaturated chain ends. Reasonably close control of

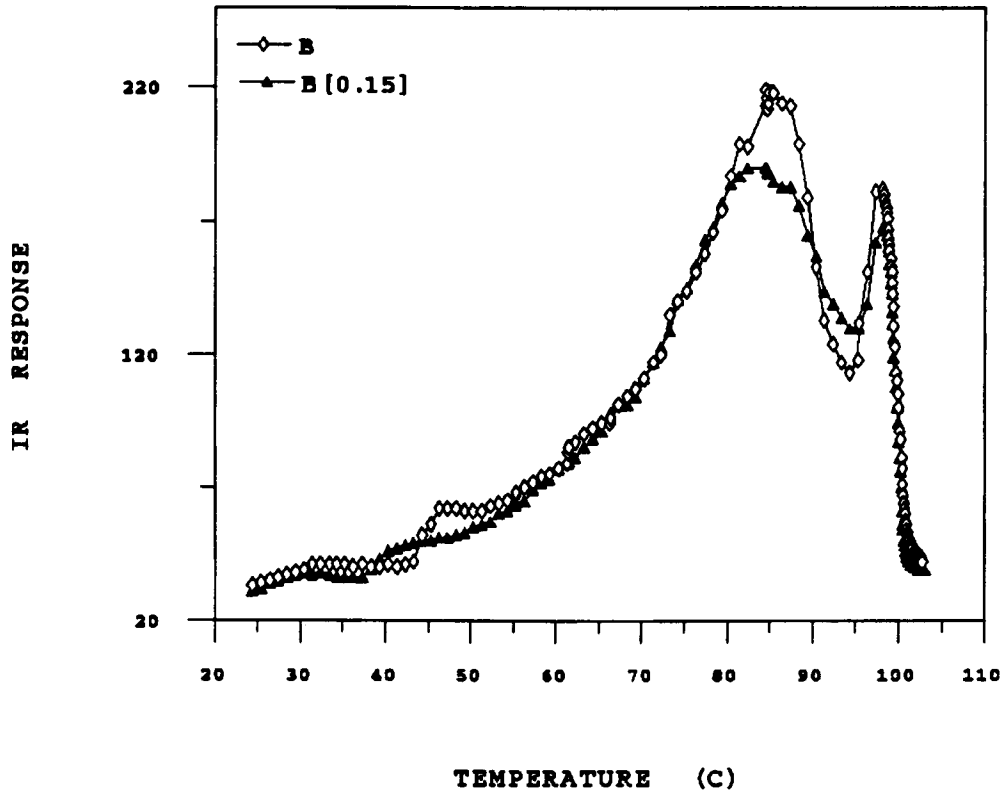

Figure 19 Analytical TREF overlays.

mixing conditions and temperature is required in order to produce consistent products. Peroxide levels about 0.15% on the PE result in mean long-branch concentrations similar to those in common LDPEs, with the mixing and extrusion equipment used in this research.

This research was supported by the Natural Science and Engineering Research Council of Canada. M. L. is grateful to CNPQ and Petrobras for scholarship support. The Ontario Centre for Materials Research funded some of the equipment used in this research.

REFERENCES

1. D. L. Cooke and M. Koyich, *SPE Antec,* **49,** 206 (1991).
2. L. A. Utracki, *Polymer Alloys and Blends; Thermodynamics and Rheology,* Hanser, New York, 1989.
3. D. Huizenga, K. Chornoby, and P. E. Engelmann, *J. Plast. Film Sheeting,* **6,** 318 (1990).
4. T. Engel, *Plast. Polym.,* **1**(38), 174 (1970).
5. T. R. Manley and M. M. Qayyum, *Polymer,* **13,** 587 (1972).
6. M. Dorn, *Adv. Polym. Technol.,* **5**(2), 87 (1985).
7. E. M. Kampouris and A. G. Andreopoulos, *J. Appl. Polym. Sci.,* **34,** 1209 (1987).
8. S. Pang and A. Rudin, *J. Appl. Polym. Sci.,* **46,** 763 (1992).
9. A. Rudin, V. Grinshpun, and K. F. O'Driscoll, *J. Appl. Polym. Sci.,* **29,** 1071 (1984).
10. A. Rudin, V. Grinshpun, and K. F. O'Driscoll, *J. Liq. Chrom.,* **7,** 1809 (1984).
11. A. Rudin, V. Grinshpun, and K. F. O'Driscoll, *ACS Symposium Series,* 245, American Chemical Society, Washington, DC, 1984, pp. 273–280.
12. L. I. Kulin, N. L. Meijerink, and P. Starck, *Pure Appl. Chem.,* **60,** 1404 (1988).
13. S. Pang and A. Rudin, *Polymer (Lond.),* **33,** 1949 (1992).
14. S. Pang and A. Rudin, in ACS Symposium Series 521, T. Provder, Ed., American Chemical Society, Washington, DC, 1993, p. 254.
15. P. van Ballegooie and A. Rudin, *Polym. Eng. Sci.,* **28,** 1434 (1988).
16. E. Karbashewski, L. Kale, A. Rudin, W. J. Tchir, D. G. Cook, and J. O. Pronovost, *J. Appl. Polym. Sci.,* **44,** 425 (1992).
17. W. T. Bremner, PhD Thesis, Department of Chemistry, University of Waterloo, 1992.
18. G. J. Ray, J. Spanswick, J. R. Knox, C. Serres, and J. C. Randall, *Macromolecules,* **14,** 1323 (1981).
19. E. T. Hsieh and J. C. Randall, *Macromolecules,* **15**(2), 353 (1982).
20. J. C. Randall, ACS Symposium Series 142, A. E. Woodward and F. A. Bovey, Eds., American Chemical Society, Washington, DC, 1980, p. 94.
21. J. C. Randall, *J. Polym. Sci. Polym. Phys. Ed.,* **11,** 275 (1973).
22. D. L. Wilfong and G. W. Knight, *Polym. Mater. Sci. Eng.,* **61,** 743 (1989).
23. D. C. Bugada and A. Rudin, *Eur. Polym. J.,* **23,** 809 (1987).
24. J. Haslam, H. A. Willis, and D. C. M. Squirrel, *Identification and Analysis of Plastics,* Butterworth, London, 1972, pp. 369–370.
25. A. Hölmstrom and E. M. Sörvik, *J. Polym. Sci.,* **18,** 761 (1974).
26. B. H. Zimm and W. H. Stockmayer, *J. Chem. Phys.,* **17,** 1301 (1949).
27. V. Grinshpun, A. Rudin, K. E. Russell, and M. V. Scammell, *J. Polym. Sci. Polym. Lett. Ed.,* **24,** 1171 (1986).
28. D. C. Bugada and A. Rudin, *Eur. Polym. J.,* **11,** 847 (1987).
29. B. H. Bersted, *J. Appl. Polym. Sci.,* **30,** 3751 (1985).
30. P. J. Hendra, A. J. Peacock, and H. A. Willis, *Polymer,* **28,** 705 (1987).
31. M. Lazär, R. Rado, and J. Rychly, in *Advances in Polymer Science,* Springer-Verlag, Berlin, Heidelberg, New York, 1990, Vol. 95, pp. 149–193.
32. T. Bremner and A. Rudin, *Plast. Rubb. Proc. Appl.,* **13,** 61 (1990).
33. T. Bremner, A. Rudin, and S. Haridoss, *Polym. Eng. Sci.,* **32,** 939 (1992).
34. D. P. McMillen and D. M. Golden, *Annu. Rev. Phys. Chem.,* **33,** 493 (1982).
35. W. J. Tchir, A. Rudin, and C. A. Fyfe, *J. Polym. Sci. Polym. Phys. Ed.,* **20,** 1443 (1982).
36. R. Amin Sanayei, K. F. O'Driscoll, and A. Rudin, in ACS Symposium Series 521, T. Provder, Ed., American Chemical Society, Washington, DC, 1993, p. 103.
37. J. C. Randall, F. J. Zoepfl, and J. Silverman, *Makromol. Chem. Rapid Commun.,* **4,** 149 (1983).
38. F. Horii, Q. Zhu, and R. Kitamaru, *Macromolecules,* **23,** 977 (1990).
39. Q. Zhu, F. Horii, R. Kitamura, and H. Yamaoka, *J. Polym. Sci. Polym. Chem. Ed.,* **28,** 2741 (1990).

Received February 21, 1995
Accepted June 6, 1995